The University of Tehran Press

Pollution

Print ISSN: 2383-451X
Online ISSN: 2383-4501

https://jpoll.ut.ac.ir/

Removal of Congo Red by Waste Fish Scale: Isotherms, Kinetics, Thermodynamics and Optimization Studies

Tapas Kumar Roy | Anupam Mondal | Naba Kumar Mondal

Environmental Chemistry Laboratory, Department of Environmental Science, The University of Burdwan, West, Bengal, India

Article Info

Article type:
Research Article

Article history:
Received: 26 June 2023
Revised: 15 December 2023
Accepted: 17 Deceber 2023

Keywords:
Adsorption kinetics
Biosorption
Central composite design
Fish scale char
Regeneration

ABSTRACT

Cong-red dye is a precursor of various products of cotton industry and its toxicity in the aquatic environment is a great concern. Present study was highlighted on the efficacy of the fish scale char (FSC) towards removal of congo red from aqueous solution. The prepared FSC was characterized by zero point charge (pHZPC), scanning electron micrograph with elemental analysis (SEM-EDX) and fourier transform infrared (FTIR). Based in the equilibrium and kinetic study, the Langmuir ($R^2 = 0.967$) and Pseudo-second-order ($R^2 = 1.00$) models are appropriate to describe the dye adsorption process. The randomness and exothermic nature of the system were confirmed by the negative values of both entropy and enthalpy, respectively. Finally, optimization by Response Surface Methodology (RSM) study revealed that the experimental data were nicely fitted with central composite design with very high F value ($F = 1596.24$, $p < 0.0001$). Perturbation plot suggested that congo-red dye removal is more sensitive with respect to biosorbent dose, pH and initial concentration. The exhausted adsorbent was regenerated with 0.5(M) NaOH solution. Therefore, it can be concluded that fish scale char could be a valuable materials towards purification of industrial effluent.

Cite this article: Kumar Roy, T., Mondal , A., & Kumar Mondal, N. (2024). Removal of Congo Red by Waste Fish Scale: Isotherms, Kinetics, Thermodynamics and Optimization Studies. *Pollution*, 10 (1), 329-347.
https://doi.org/10.22059/POLL.2023.361313.1963

DOI: https://doi.org/10.22059/POLL.2023.361313.1963

INTRODUCTION

Industrial effluent consists many pollutants, among them dye is an important component (Saravanan et al., 2021). However, few specific industries such as pulp and paper, cotton, pharmaceuticals, etc. are the major contributors of dye containing pollutants (Islam et al., 2019). Dyes are various types such as azo and non-azo dyes. Dyes causes many problems including prevention of sun light which again cause low primary productivity and disturb the COD/BOD level in aquatic medium (Karimifard & Moghaddam, 2018). Again, Azo dyes have carcinogenic azo bond (-N=N-) which causes cancer. Various techniques have been employed to overcome from dye pollution such as coagulation, reverse osmosis, precipitation, adsorption etc. However, adsorption is the best technique over other available techniques because of low operation cost and minimum sludge generation (Karaman et al., 2022). Previous researchers used many adsorbents for the removal of congo red such as calcium-rich fly ash (Acemioglu, 2004), bagasse fly ash (Mall et al., 2005), untreated bottom ash (Saleh et al., 2012), fly ash/$NiFe_2O_4$ composites (Govindaraj et al., 2018), Industrial waste (Harja et al., 2022), zeolite/algae composite [10], *Padina gymnospora* (Dryaz et al. 2021), fish scale (Jaafar et al., 2022) etc. However, use of fish scale char is very scanty with respect to removal of congo-red dye.

*Corresponding Author Email: nkmenvbu@gmail.com

Fish scale consist a valuable protein called collagen which supposed to be responsible for adsorption of dyes (Kabir et al., 2019). Collagen has various amino acids which bind each other to form a triple helix known as collagen helix and mostly available in connective tissue. However, fish scale also consists an inorganic substance known as hydroxyapatite which is also responsible for binding of various pollutants (Zhu et al., 2013). Previous research highlighted the extensive uses fish scale as an efficient adsorbent for decontamination of toxic dyes such as reactive red 2, reactive orange 16, reactive blue 5G, methylene blue etc. (Begum & Kabir, 2013; Marrakchi et al., 2017; Neves et al., 2018). But, very limited research are there where fish scale char was used for dye removal. From this backdrop, present work was performed through conversion of fish scale char from raw fish scale followed by characterization through $pH_{ZPC,}$ $_{SEM-EDX}$ and FTIR and same was used to remove to anionic dye, congo-red through batch process followed by optimization study with response surface methodology.

MATERIALS AND METHODS

Adsorbent preparation

Fish scale Char (FSC)

The raw fish scales (*Labeo rohita*) were collected from a local fish market in Burdwan. The material was washed repeatedly with deionized distilled water to remove soluble impurities from their surface. The fish scales were allowed to sundry for 15-20 days. The scales were then kept in muffle furnace initially at 250ºC to maximum at 650ºC for long range of time (12 h). The residue was grounded and sieved through 250 µm screen. The sieved fish scale char (FSC) were stored in sterile, air-tight glass container and used as an adsorbent.

Adsorbent characterization

The prepared adsorbent was characterized by various analytical instruments. Point of zero charge ($pH_{zpc)}$ on the surface of the adsorbent was measured by following the method as explained by (Debnath & Mondal, 2020). On the other hand, surface morphology of the adsorbent both before and after adsorption were assessed by scanning electron microscopy with EDX (Zeiss Sigma 300) and the various functional groups those are associated on the surface of the adsorbent was evaluated by Fourier transform infrared spectroscopy (FTIR) (Agilent 650).

Experimental design

A stock solution (500 mg/L) of congo red dye was prepared and intermediated solutions (50, 100, 150, 200 and 250 mg/L) were prepared through proper dilution method (Roy et al., 2022). The operating variables such as initial concentration of congo red dye (50-250 mg/L), adsorbent dose (0.2 – 2.0 g/100 mL), pH (5-10), contact time (5-120 min) and temperature (293-363 K) were maintained during batch study. Finally, the residual dye concentration was measured through spectrophotometric method (λmax = 497) (Wekoye et al., 2020).

Dye removal efficiency

After batch adsorption, the residual dye concentration was evaluated by following the equation:

$$Dye\ removal\ (\%) = \frac{(C_0 - C_e)}{C_0} \times 100$$

Similarly, the adsorption capacity was measured by following the equation:

$$Adsorption\ capacity\ (mg/\mathrm{g}) = \frac{(C_0 - C_e)}{m} \times V$$

Where C_o and C_e are the initial and equilibrium dye concentration (mg/L), respectively and m is the mass (g) of the adsorbent and V (L) is the volume of dye taken for the batch study.

Statistical optimization

In order to find out the optimization of the congo red dye adsorption, response surface methodology (RSM) (Design Expert® 7.0) was performed. Mathematical modelling of Box–Behnken design of RSM was considered (Nguyen et al., 2022). RSM is mainly based on the collective contribution of mathematical and statistical methods (Khedmati et al., 2017) where experimental outcomes are fitted in linear, square polynomial functions etc. and the verification of the models will be established through statistical techniques (Witek-Krowiak et al., 2014). The optimal conditions will be screened from RSM through following some basic steps such as selection of variables or factors and expected responses, selection of experimental design, running the experiment and recording results, experimental data will be fitted for getting mathematical model, confirmation of model through the analysis of variance and finally, determine the optimal conditions (Karimifard & Moghaddam, 2018).

RESULTS AND DISCUSSION

Physical characterization of Fish scale char

Physical Characteristics

The zero point charge (pH_{zpc}) of FSC was determined and presented in Figure 1a. From the Figure 1a, it is clear that pH_{ZPC} of the fish scale char is 7.6 and high anion exchange capacity revealed that FSC can exhibit good adsorptive nature of CR dye.

FTIR spectral analysis of FSC

The adsorption capacity of fish scale char depends upon the binding capability of the different functional groups on its surface. Therefore, it is important to know the internal structure as well as insight of adsorption nature of fish scale char. Several peaks were observed from the spectra (Fig. 1b) indicating that fish scale char is composed of various functional groups which are responsible for chemical attachment with the anionic azo dye CR. The FTIR spectral analysis of fish scale char powder shows distinct peaks at 798.0, 963.0, 2865.5, 2932.0, 3409.0 cm^{-1} (Fig. 1b). Within the region 1559-1660 cm^{-1}, the absorption band indicates the overlapping of the (-C=C-) stretching vibration mode of the aromatic ring of the carbon with the (-C=O) absorption bands of carboxylic, ester, lactone, and carbonyl groups (Kabir et al., 2019). The peak observed at 3409.25 and 2865.00 cm^{-1} may be assigned to the presence of alcohol hydroxyl group (-OH) and acidic hydrogen group (-OH) stretching respectively (Bhaumik et al., 2011; Das & Mondal, 2011).

SEM-EDAX study

The study of scanning electron micrograph with elemental analysis is extremely important for proper understanding the surface morphology of the adsorbent (Han et al., 2021). Figure 1c-d, highlighted that the SEM of fish scale of char of before and after dye adsorption, respectively. The surface of FSC was smooth with few impurities, but after adsorption, the surface of the adsorbent is not smooth enough (Fig. 1c and d). Similarly, EDAX study revealed that there is sharp variation of elemental composition (Fig. S1a and b).

Batch studies of adsorption of CR removal onto FSC

Effect of initial concentration

The impact of initial dye concentration under fixed amount of adsorbent along with constant pH, contact time and temperature on the percentage of removal was represented in Fig. 2a.

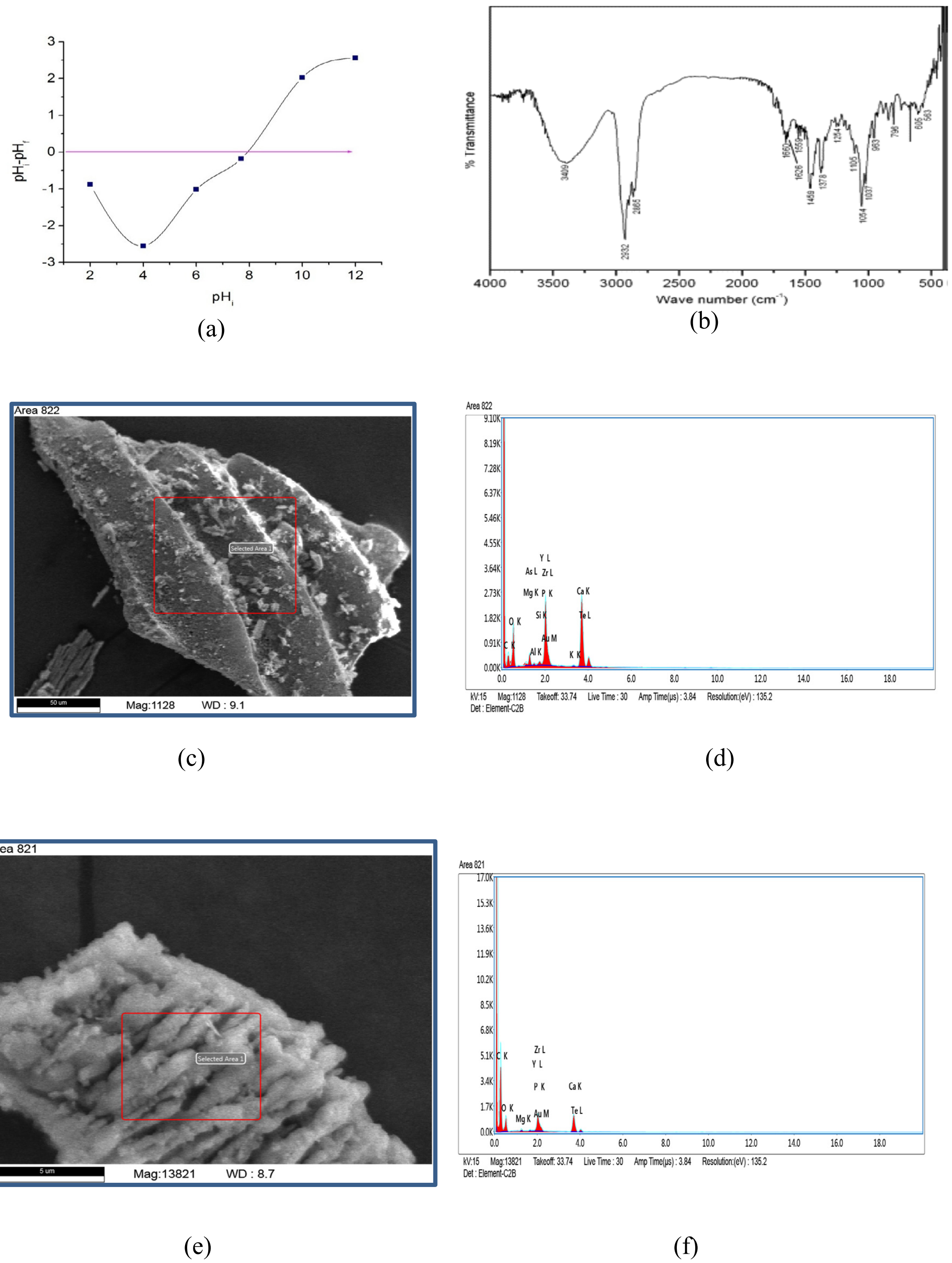

Fig. 1. (a) Zero point charge of FSC, (b) FT-IR of FSC before adsorption of CR, (c) SEM of fish scale before dye adsorption, (d) EDAX of fish scale before dye adsorption, (e) SEM of fish scale after dye adsorption and (f) EDAX of fish scale after dye adsorption.

Figure 2a demonstrated that the initial dye concentration was taken in the range of 50-250 mg/L and pH was adjusted to 7.0 for the biosorption of CR on FSC. The results indicated that the CR dye adsorption capacity of FSC increased from 3.91 mg/g to 19.6 mg/g with increase initial concentration (Fig. 2a). This may be due to the increase of concentration gradient which ultimately increasing the driving force to overcome all mass transfer resistances between the solution and solid phase (Wanyonyi et al., 2014). At lower initial concentration, the percentage removal was higher and reduced at higher concentration. This is perhaps due to perfect contact between dye molecule and biosorbent initial concentration. Therefore, it can be finalized that at high concentration, the percentage of removal was high due to the lower ratio between available CR dye and adsorption CR dye whereas. But, the percentage of removal became low due to unavailability of vacant adsorbent sites where dye molecules may binds (Mondal et al., 2023).

Effect of adsorbents dose

The effect of biosorbent dose on the CR adsorption from aqueous solution is investigated. The adsorption capacity and removal efficiency were observed at different significant variation of biosorbent dosages (0.25-1.25 g for 100 mL solution). The removal of CR was studies at different doses 0.25-1.25 g for 100 mL solution by keeping the contact time 30 min., pH 8, concentration 100 mg/L. It is apparent from Fig. 2b that the removal process was increased from 71.11% to 87.5% when FSC dose was increased from 0.25 to 1.0 g for 100 mL solution. It is perhaps due to that the availability of active sites and surface area increased by increasing the adsorbent dose (Sen & Mondal, 2022). However, no remarkable removal of CR dye was recorded above 1.0 g/100 mL. It is again due to overlapping of active sites with increasing dose (Sen et al., 2021). Present finding is in accordance with earlier findings (Yadav et al., 2021; Oloo et al., 2020).

Effect of pH

The status of H^+/OH^- ions of the dye solution is a major contributing factor in dye adsorption process (Gurav et al., 2021). In the present study, pH of the dye solution was varied from 4.5 to 11. The mechanism of this adsorption i.e., interaction between dye molecules and the surface of the adsorbent could be understood from the zero point charge (pHzpc) of the adsorbent. The adsorption of CR by FSC biosorbent would be dramatically changed as the values of below and above zpc. In case of anionic dye like CR, the adsorption is favorable at pH<pHzpc due to occurring well interaction between anionic CR and cationic biosorbent (Mondal, 2010). The entire changes of the percentage of removal and the adsorption capacity are depicted in Fig. 2c. The CR adsorption rates increased with increasing pH up to 8. However, further increase of pH, dye removal efficiency decreases (Fig. 2c). It was shown that at very low and very high pH, the adsorption of CR dye was low. This is perhaps due to at low pH, the anionic is changed into neutral species and at very high pH, and both have electrostatic repulsion that is not favorable for adsorption. Present findings are corroborated with the earlier reports (Satapathy et al., 2020; Kim et al., 2020).

Effect of contact time

The investigation of the effect of contact time on the adsorotive removal of CR was depicted in Fig. 2d. The CR removal process was recorded as a function of contact time. The uptake capacity of CR dye by FSC dose was very fast and 92.31% removal was sorbed within 20 minutes and equilibrium was established after 120 minutes. Moreover, it was observed that at 30 min, almost all the CR became adsorbed. It may be explained by the abundant availability of active sites on the catalyst surface (Wekoye et al., 2020; Das et al., 2013). At the beginning, the dye removal was fast due to the availability of active sites on the adsorbent surface (Das et al., 2013; Saqib et al., 2013). However, active site of the adsorbent surface is not only depends on the surface area, but on the availability of the active dye binding sites (Kabir et al., 2019). Other previous researchers (Karimifard & Moghaddam, 2018; Januárioet al., 2021; Bannerjee & Chattopadhyaya, 2017) also suggested the same argument for their adsorption studies.

Effect of temperature

Fig. 2e indicates the effect of temperature of removal of CR onto FSC. The adsorption capacity increased up to 9.23 mg/g with increasing temperature up to 308 K. This adsorptive removal of CR is exothermic and indicating that at lower temperature, adsorption is more favorable than

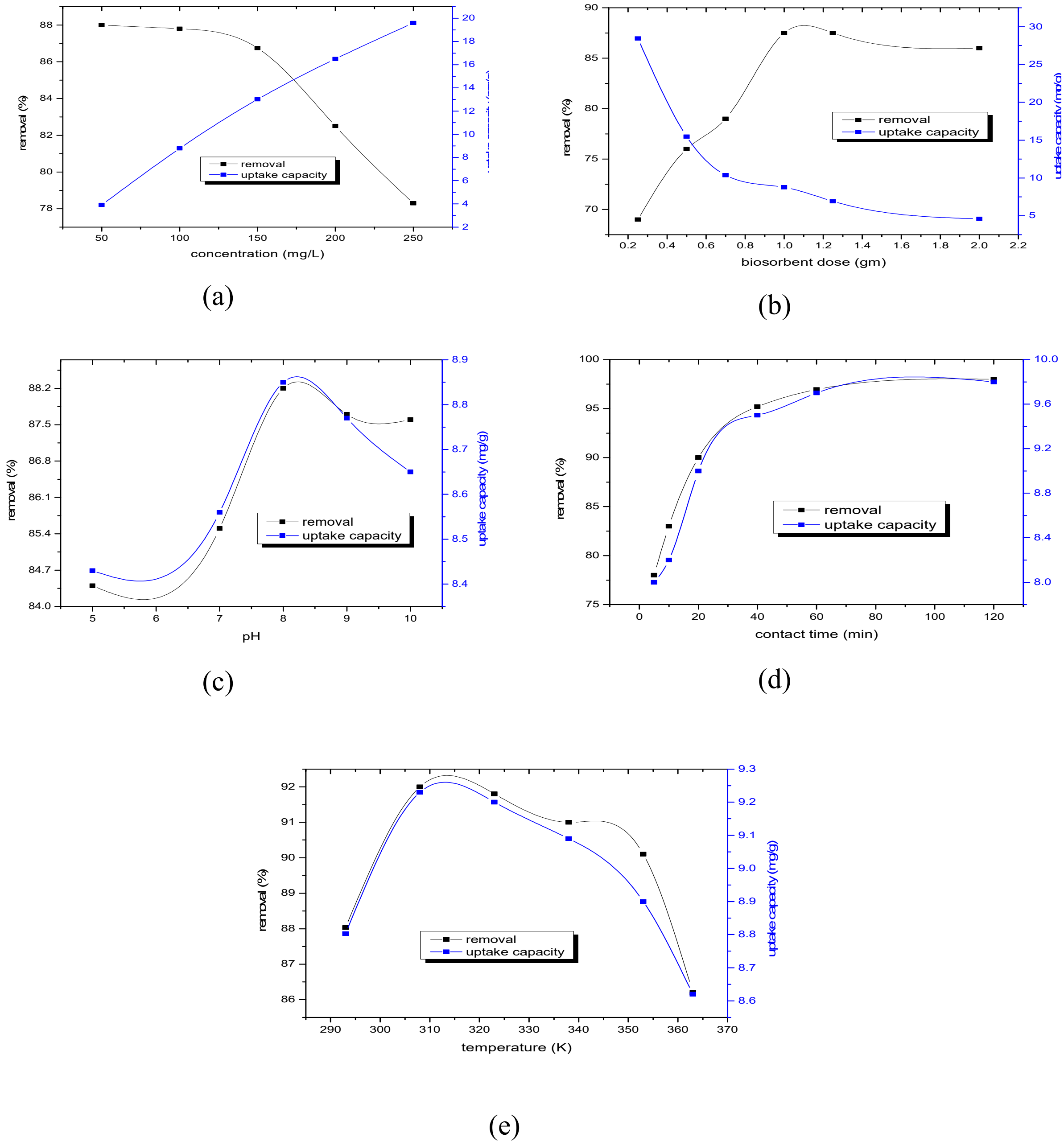

Fig. 2. (a) Effect of initial concentration on CR adsorption (experimental conditions: Initial concentration: 25 mg/L, agitation speed: 600 rpm, pH: 6.0, Temperature: 313K, Contact time: 90 min), (b) Effect of biosorbent dose on CR adsorption (experimental conditions: Initial concentration: 25 mg/L, agitation speed: 600 rpm, pH: 6.0, Temperature: 313K, Contact time: 90 min), (c) Effect of pH on CR adsorption (experimental conditions: Initial concentration: 25 mg/L, agitation speed: 600 rpm, pH: 6.0, Temperature: 313K, Contact time: 90 min), (d) Effect of contact time on CR adsorption (experimental conditions: Initial concentration: 25 mg/L, agitation speed: 600 rpm, pH: 6.0, Temperature: 313K, Contact time: 90 min) and (e) Effect of temperature on CR adsorption (experimental conditions: Initial concentration: 25 mg/L, agitation speed: 600 rpm, pH: 6.0, Temperature: 313K, Contact time: 90 min).

higher temperature. The increase in CR adsorption with rise in temperature could be attributed to the endothermic nature of dye adsorption (Vyavahare et al., 2019).

Equilibrium isotherms

The nature of a specific adsorption phenomenon was diagnosed by the equilibrium isotherm data. The experimental adsorption data were described by the equilibrium isotherm model. The sorption mechanism and the surface properties and affinity of the adsorbent were explained by using this equilibrium model (Table 1). The equilibrium relationship between the biosorbent surface and dye concentration in liquid phase are investigated by isotherm study. Similarly, the determination of the extent to that material can be sorbed onto biosorbent surface. Therefore, the establishment of the most appropriate isotherm model for the determination of equilibrium data and evaluating the applicability of the adsorption process, isotherm studies were very essential. Here four isotherms like Langmuir, Freundlich, Temkin and D-R isotherm were applied to determine the sorption data (Fig. S1a-d). The linear form of Langmuir isotherm gives a significant fit isotherm which is more accurate for the adsorption system design (Fig. S1a). The Langmuir isotherm supports a monolayer adsorption onto a homogeneous surface (Gurav et al., 2021). The maximum monolayer adsorption capacity of Langmuir model was found to be 33.33 mg/g.

The next important isotherm is Freundlich isotherm which can be measured the 1/n value confirming the favorability of adsorption (Fig. S1b) (Çelekli et al., 2019). The value of 1/n less than 1describe a favorable adsorption process (Table 1). The Temkin model did not fit well with experimental data by comparing the Langmuir and Freundlich isotherm. The adsorption binding energy for CR of Temkin isotherm was recorded 8.87 KJ/mol (Fig. S1c). The D-R adsorption energy i.e, the estimated value of E is 132.11 J/mol Fig. S1d). The estimated value of *E* (< 8 kJ/mol) has been indicated toward the physisorption process (Das et al., 2013). Therefore, it can be concluded that this physisorption process will play an important role for the biosorption of CR on to FSC (Dada et al., 2012; Samarghandi et al., 2009).

Biosorption kinetics

The uptake rate of sorbate which in turn controls the residence time of the sorbate at the solid–solution interface including the diffusion process is described by the kinetics of any adsorption process. The study of kinetics of CR adsorption helped to obtain the kinetic data.

Table 1. Isotherm data for adsorption of CR dye by fish scale charcoal (FSC)

Adsorption isotherm	Equations	Parameters (unit)	Values	R^2
Langmuir isotherm	$\frac{1}{q_e} = \frac{1}{q_{max}K_LC_e} + \frac{1}{q_{max}}$	$q_{max}(mg/g)$ K_L (L/mg)	33.33 0.0241	0.967
Freundlich isotherm	$\log q_e = \log k_F + \frac{1}{n}\log C_e$	K_F (mg/g)(L/mg)$^{1/n}$ n	0.424 3.90.92	0.960
Temkin Isotherm	$q_e = \frac{RT}{b_T}(\ln A_T + \ln C_e)$	A_T (L/mg) b_T (KJ/mol)	0.181 8.87	0.983
D - R isotherm	$\ln q_e = \ln q_{max} - \frac{1}{2E^2} \times \left[RT\ln\left(1+\frac{1}{C_e}\right)^2\right]$	$q_{max}(mg/g)$ E (J/mol)	20.19 132.41	0.923

Where q_{max} is the maximum adsorption capacity; K_L, K_F, A_T and b_T are different adsorption constants; n is the heterogeneity factor; E is the mean free energy of adsorption per mole of the adsorbate; T is the temperature (K), and R is the ideal gas constant (8.3145 J/mol K).

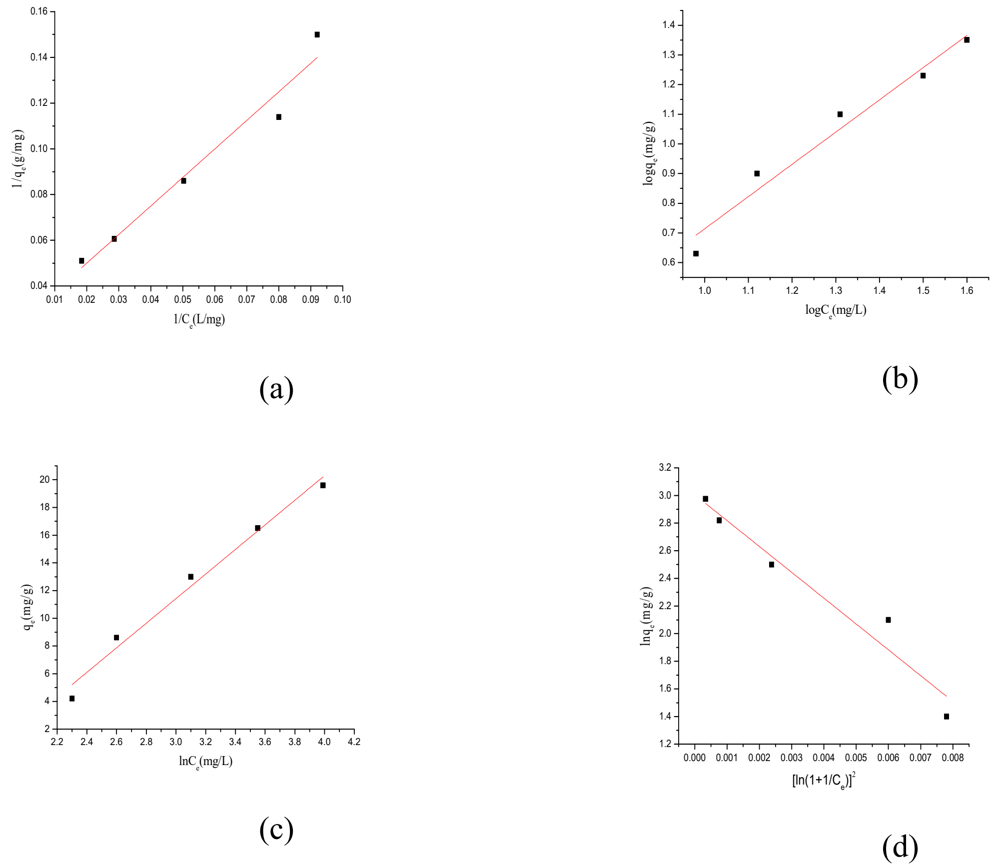

Fig. S1. (a) Langmuir isotherm study for adsorption of CR onto FSC, (b) Freundlich isotherm study for adsorption of CR onto FSC, (c) Temkin isotherm study for adsorption of CR onto FSC, and (d) D-R isotherm study for adsorption of CR onto FSC.

Table 2. Summary of parameters for various kinetic models

Kinetic model	Equations	Parameters(unit)	Values	R^2
Pseudo first- order	$\ln(q_e - q_t) = \ln q_e - K_1 t$	q_e (mg/g) K_1 (min^{-1})	2.4 0.055	0.975
Pseudo second-order	$\frac{t}{q_t} = \frac{1}{K_2 q_e^2} + \frac{t}{q_e}$	q_e (mg/g) K_2 (g/mg.min)	10 0.0617	1.0

Where q_t is the adsorption capacity at time t; k_1 and k_2 are the first-order and second-order rate constant, respectively

Here two kinetic studies like pseudo-first order and pseudo-second order models were analyzed (Figs. S2a and b). The linearized form of biosorption kinetics (Guo et al., 2022) and their constants are presented in Table 2. The linear relationship of the plot of t/q vs t which indicated that the adsorption of CR onto FSC followed the pseudo-second order reaction is represented in Figure S2b (Choi et al., 2020). The slope and intercept of plot helped to determine the values of q_e and K_2. The calculated adsorption capacity of pseudo-second order kinetic model are close to the experimental values with comparison of pseudo-first order kinetic model due to having high correlation coefficient ($R^2 = 1.0$) and excellent linearity (Table 2)(Jabar et al., 2020).

Biosorption thermodynamics

The thermal activity on biosorption process is associated with different thermodynamic parameters. It can be concluded from the thermodynamic data that whether the process is spontaneous or not (Yang et al., 2022). The spontaneity of a process was determined by the plotting of Van't Hoff equation (Fig. S2c).

$$\Delta G^0 = -RTlnK_c$$

Where R, T, and K_C are the universal gas constant, temperature (K) and distribution coefficient defined as:

$$K_C = \frac{C_a}{C_e}$$

In which C_a is the equilibrium sorbate concentration on the biosorbent (mg L^{-1}) and C_e is the equilibrium sorbate concentration in solution (mg L^{-1}).

Otherwise, ΔG^0 is the function of enthalpy (ΔH^0) and entropy (ΔS^0) according to the following equation:

$$\Delta G^0 = \Delta H^0 - T\Delta S^0$$

The plot of free energy (ΔG^0)Vs temperature (T) can be helped to determine the values of enthalpy and entropy are represented in Table 3. The most favorable biosorption process was observed at temperature of 40 ^{0}C and further increasing temperature indicates that the process was not favorable at higher temperatures. The change of enthalpy and entropy of this process can be measured by the slope and intercept of the plot (Fig. S2c). The randomness and exothermic nature of the system were confirmed by the negative values of both entropy and enthalpy respectively (Das et al., 2013). Present study results showed good agreement with earlier published report (Jawad & Abdulhameed, 2020; Vijayakumar et al., 2012).

Central composite design (CCD)

The determination of optimized set of operational parameters in removal of CR was conducted by response surface methodology (RSM). The three important independent variables viz., initial concentration, biosorbent dose and pH of CCD in RSM were used to investigate their influence on the biosorption of CR onto FSC (Karimifard & Moghaddam, 2018). The Table S1 illustrates the experimental range of the variables with their unit and notation used in CCD. The Design–Expert software (version 7.0.3 Wiley. Ink) was used to develop the central composite design.

Table 3. Thermodynamic parameters for adsorption of CR dye by FSC

Thermodynamic parameters	Equations	Values (J/mol)
Standard free energy	$\Delta G^0 = -RTlnK_c$	
293K		-194.2
308K		-281.7
323K		-104
338K		-64.6
353K		-35.2
363 K		-21.2
Standard enthalpy change	$lnK_c = \frac{\Delta S^0}{R} - \frac{\Delta H^0}{RT}$	-845.6
Standard entropy change		-2.23

Where K_C is the equilibrium constant; T and R are as Kelvin temperature and molar gas constant respectively.

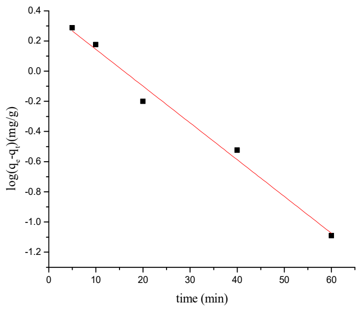

(a)

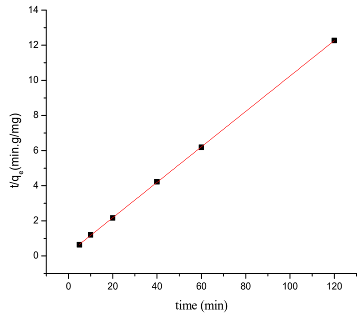

(b)

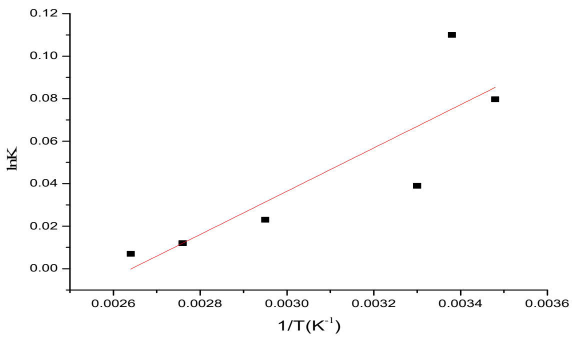

(c)

Fig. S2. (a) 1st order kinetic for adsorption of CR on FSC, (b) 2nd order kinetic for adsorption of CR on FSC and (c) Thermodynamic study for adsorption of CR onto FSC.

Table S1. Variables and levels considered for the adsorption of CR onto Fish Scale charcoal(FSC).

Name(factor)	Units	Low	High
Initial concentration(X_1)	ppm	50	100
dose(X_2)	gm	0.25	2.0
pH(X_3)		5	10

Evaluation of the fitting process model and ANOVA

The detection and suggestion of CCD model was validated by the fitting of existing linear, two factor interactions (2FI), cubic and quadratic model. Table S2 and S3 represents the quadratic model that was selected to continue the progress. A few number of statistical evidences in the ANOVA analysis were further confirmed a valid quadratic model (Table 4). The Fisher variation ratio (F), probability value (p-value), lack of fit, the different coefficient of R-squared values and adequate precision are the different evidence of CCD model. A signal to noise ratio is known by adequate precision. It compares the range of the predicted values at the design points to the average prediction error. The measurements of the amount of variation around the mean and new explained data were confirmed by values of Adj R^2 and Pred R^2 (Table S3). The degree of significance of each variable was declared by the p-value while *F*–value is a statistically valid measure of how well the factors describe the variation in the data about its mean (Chattoraj et al., 2014; Roy et al., 2014; Kumar & Phanikumar, 2013). The presence of high *F*–value (1596.24), very low *p*–value (< 0.0001), non– significant lack of fit, the high coefficient of *R*–squared (0.999), adjusted *R*– squared (0.999), predicted *R*–squared (0.999) and the adequate precision (104.78) (Table S3). The actual values versus predicted values of the adsorption of CR are depicted in Figure 3. The excellent agreement between actual and

Table 4. Analysis of variance (ANOVA) for percentage removal of Congo Red onto fish scale charcoal (FSC).

Source	Sum of Squares	Mean df	F Square	p-value Value	Prob > F	
Model	18285.12	9	2031.68	1596.24	< 0.0001	significant
A-concentration	1405.93	1	1405.93	1104.61	< 0.0001	
B-dose	9260.64	1	9260.64	7275.86	< 0.0001	
C-pH	2.66	1	2.66	2.09	0.1787	
AB	144.50	1	144.50	113.53	< 0.0001	
AC	180.50	1	180.50	141.81	< 0.0001	
BC	112.50	1	112.50	88.39	< 0.0001	
A^2	5.80	1	5.80	4.56	0.0585	
B^2	1772.18	1	1772.18	1392.36	< 0.0001	
C^2	6665.28	1	6665.28	5236.75	< 0.0001	
Residual	12.73	10	1.27			
Lack of Fit	12.23	9	1.36	2.72	0.4409	not significant
Pure Error	0.50	1	0.50			
Cor Total	18297.85	19				

Table S2. Adequacy of the model tested.

Source	Sum of Squares	df	Mean Square	F Value	p-value	Prob > F
Mean vs Total	79872.16	1	79872.16			
Linear vs Mean	9650.89	3	3216.96	5.95	0.0063	
2FI vs Linear	437.50	3	145.83	0.23	0.8732	
Quadratic vs 2FI	8196.74	3	2732.25	2146.66	< 0.0001	Suggested
Cubic vs Quadratic	4.12	7	0.59	0.21	0.9612	Aliased
Residual	8.61	3	2.87			
Total	98170.01	20	4908.50			

Table S3. Model summary statistics for Congo Red adsorption onto fish scale charcoal(FSC).

Source	Std. Dev.	R-Squared	Adjusted R-Squared	Predicted R-Squared	PRESS	
Linear	23.25	0.5274	0.4388	0.2598	13543.84	
2FI	25.13	0.5513	0.3443	-0.1252	20589.07	
Quadratic	1.13	0.9993	0.9987	0.9989	20.84	Suggested
Cubic	1.69	0.9995	0.9970		+	Aliased

predicted values of this graph indicates a valid model.

The empirical relationships have been expressed in terms of unit less regression coefficient by the quadratic model is given by the following coded factor equation:

$$Y = +86.04 - 10.61x_1 + 27.97x_2 - 0.44x_3 - 0.71x_1^2 - 13.11x_2^2 - 21.43x_3^2 - 4.25x_1x_2 + 4.75x_1x_3 + 3.75x_2x_3$$

A regression analysis of the model equation (Table 4) shows that the main as well as the interaction effects of initial concentration, biosorbent dose and pH were highly significant ($p <$ 0.0001).

Interaction of variables

In the present study, the interaction among different independent parameters and their

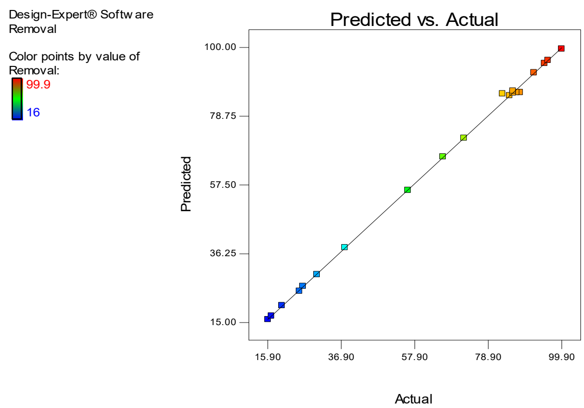

Fig. 3. Actual vs Predicted plot of CCD model of RSM for CR removal.

individual effect on biosorption of CR onto FSC were depicted in Figures 4a-f. The 3D surface and contour plot are the representation of the response surface as a three and two dimensional plane (Fig. 4a, c and e and 4b, d and f). This analysis realize that the influence of which parameters have a better interaction among them. The 3D plot and contour plots of the combined effect of initial concentration with biosorbent dose and pH have been presented in Fig. 4a and b. The percentage removal of CR decreases with increase in both the initial concentration and biosorbent dose due to having limited number of active sites on biosorbent (Das et al., 2013; Chowdhury et al., 2013). The combined effect of pH with both initial concentration and biosorbent dose for continuous adsorption of CR are depicted in Figures 4c-f. From the observation of contour and 3D surface plots, the maximum removal were obtained to 99.90% at optimized condition of initial concentration (150 ppm) and biosorbent dose (1.13 g).

Perturbation plot

The individual effect of process parameters like initial concentration, biosorbent dose and pH on removal of CR onto FSC were evaluated by perturbation plots (Fig. 5a). It was treated as a one factor-at-a-time experimentation. The individual effect of all independent variables at a particular point in the design space was compared by perturbation plots (Fig. 5b). The response of one factor is graphically represented by changing only one factor over its range while holding the other factors constant. A steep slope or curvature in a factor shows that the response is sensitive to that factor (Roy et al., 2014; Sadhukhan et al., 2014). Figure 5a also shows that the removal of CR is more sensitive to biosorbent dose followed by initial concentration and pH.

Optimization using the desirability functions

The maximize, minimize, target, in range and set to an exact value of response are the possible goals in the Design–Expert software‘s. In numerical optimization, each variable and response from menu preferred the desired goal (Kumar & Phanikumar, 2013; Chowdhury et al., 2013). The criterion of desirability values of the optimization procedure was demonstrated by a set as maximum for initial concentration, minimum for FSC dose, in range for pH and the goal for maximum which analyze the optimal condition of the variables (Fig. 5b). The maximum removal for low biosorbent dose was the main objective of this process. In this, the desirability value ranges from 0.962 to 1 for individual variables and 0.981 for combination of all the variables. The optimized result obtained from CCD coincides well with experimental value, suggesting that the FSC may be an effective and economically feasible biosorbent for the removal of CR from water.

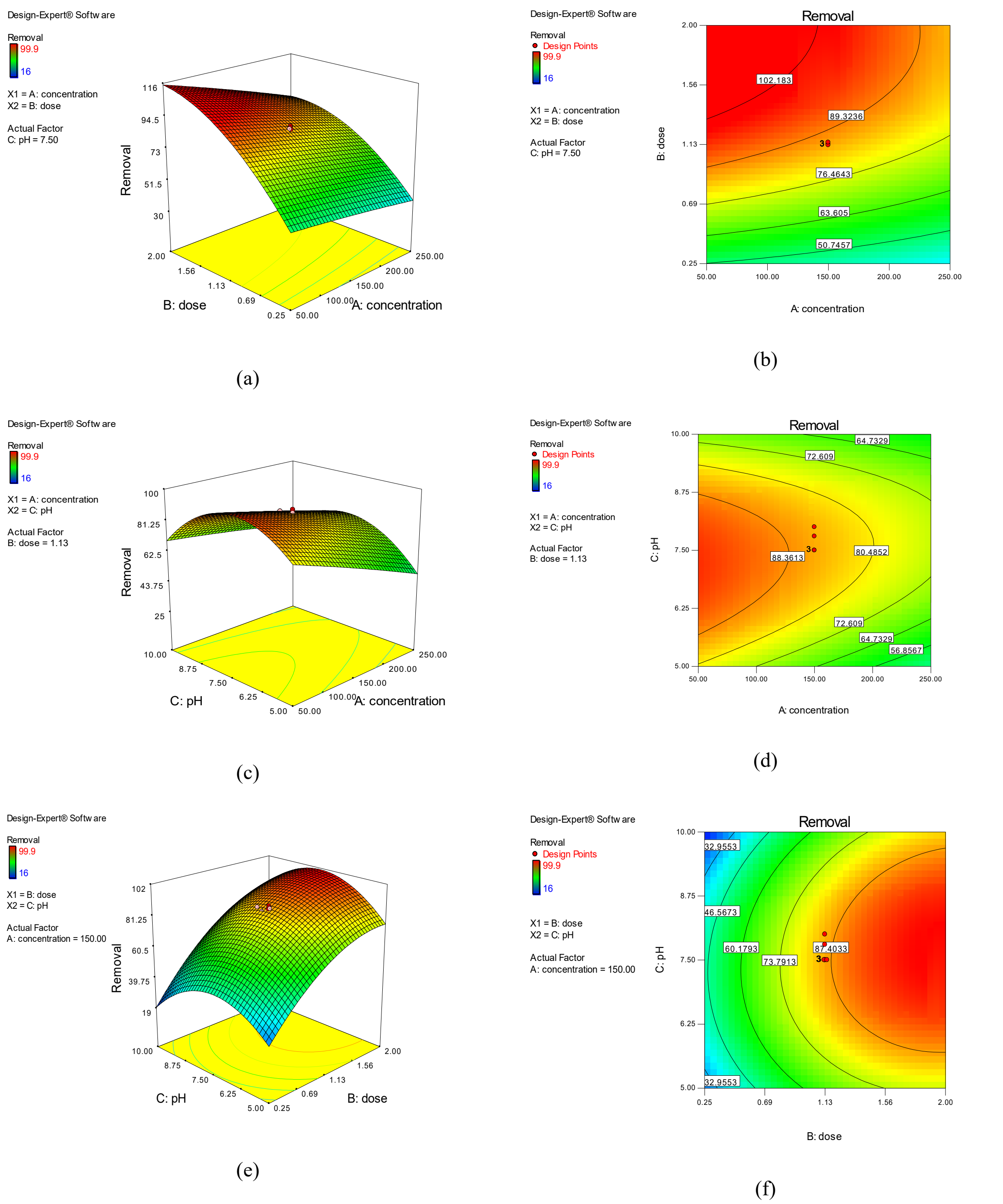

Fig. 4. 3D surface and contour plot of combined effect between dose and concentration (a) and (b), combined effect between pH and concentration (c) and (d), and combined effect between dose and pH (e) and (f).

Simulated interaction mechanism

The surface of fish scale char consists many functional groups such as carbonyl group, hydroxyl group and carbon-carbon unsaturation which may strongly interacted with congo red dye molecules (Fig. 6). This interactions are mainly electrostatics in nature (Jaafar et al., 2022). The congo red dye has many areas such as azo (–N=N-), sulphite (-SO_3) and amine (-NH_2) groups which directly involved in the interaction with active functional groups of fish scale char (Jaafar et al., 2022).

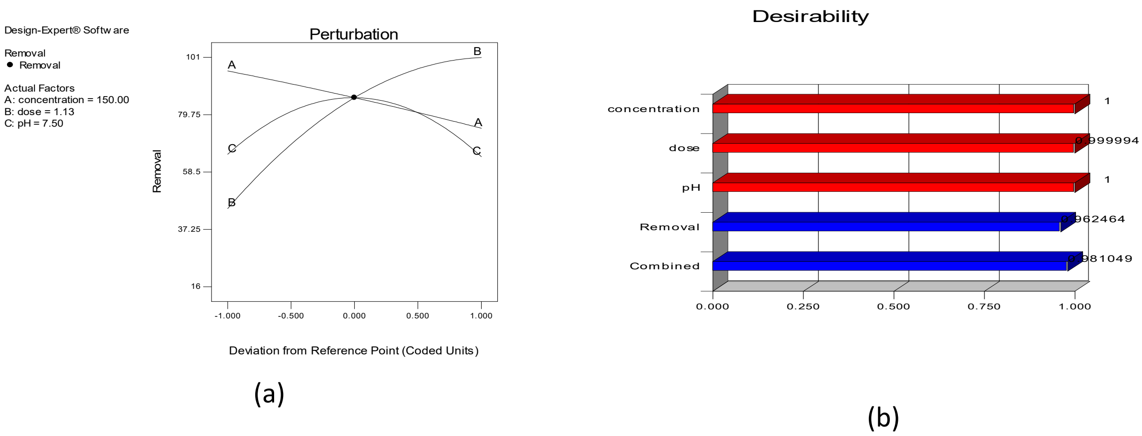

Fig. 5. (a) perturbation plot of variables used in RSM, and (b) Desirability bar plot of CCD model of RSM for CR removal.

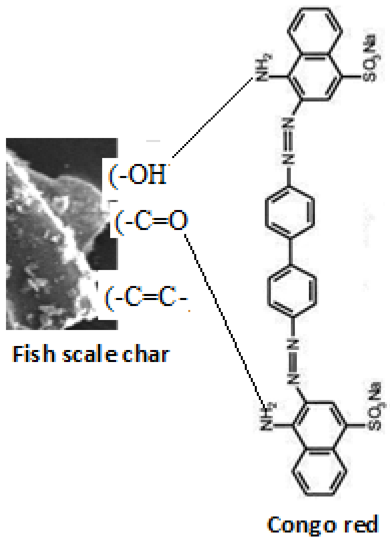

Fig. 6. Simulated mechanism showing interaction between various functional groups of fish scale char and congo red dye molecule.

Desorption studies

A successful adsorption process operation requires multiple reuses of the adsorbent that greatly reduces the process cost and also decreases the dependency of the process on a continuous supply of adsorbents (Ranjan et al., 2009; Vijayaraghavan et al., 2009). Desorption studies are required to reuse the CR-loaded FSC biomass for further treatment of waste water. The recovery of biosorbent was conducted by the different concentration of NaOH solution (Figure not provided). It can be shown that with increase the strength of NaOH solution from 0.5 to 4 M, CR desorption percentage increased from 25 - 88 %. So after desorption experiment, a significant amount of FSC biomass can be effectively reused. Almost similar results was reported by Sadhukhan et al. (2016).

Comparative study

In order to compare the adorption capacity of the studied adsorbent with previous studies, a comprehensive Table is provided (Table 5). From the Table 5 it is clear that various adsorbents

Table 5. Comparison of adsorption capacities of various adsorbents for CR.

Adsorbent	q_{max}(mg/g)	References
Calcium-rich fly ash	9.41	Acemioglu, 2004
Bagasse fly ash [BFA]	11.885	Mall et al., 2005
Carbon from Jujube (*Ziziphus mauritiania*)	0.182	Aminu et al., 2020
Fly ash (industrial waste)	22.12	Hajra et al., 2022
Fly ash/$NiFe_2O_4$ composites	22.73	Sonar et al., 2014
Fish scale char	33.33	Present work

were used for the removal of congo red from aqueous medium. However, all the adsorbents showed low to moderate adsorption capacity ranges from 0.182 to 22.73 mg/g. Only two adsorbents, fly ash (industrial waste) and fly ash/$NiFe_2O_4$ composite showed the adsorption capacity as 22.12 mg/g and 22.73 mg/g, respectively and these two are much lower adsorption capacity than the present studied adsorbent (33.33 mg/g). Therefore, it may be suggested that the present adsorbent is more efficient than the previous adsorbent used for the removal of congo red dye.

CONCLUSION

Present research highlighted to eliminate congo red dye from aquatic medium through batch adsorption process by fish scale char. The synthesized adsorbent was characterized by various analytical instruments (FTIR, SEM and EDX). Finally, optimized condition for maximum adsorption was evaluated through response surface methodology and optimal parameters are …. The adsorption isortherm, thermodynamic and kinetic analysis revealed monolayer homogeneous nature, spontaneous, exothermic and chemisorption nature of dye adsorption. The exhausted adsorbent was regenerated with alkali treatment. Therefore, fish scale waste could be an efficient inexpensive biomaterial for removal dye from aqueous medium. Future study should be focus to enhance the adsorption capacity of fish scale char by introducing various techniques of char preparation along with mixing of various nanomaterial. Moreover, as fish scale is a low-cost easily available raw material, it could be used in the treatment of contaminated industrial waste water on a large-scale.

ACKNOWLEDGEMENTS

The authors express there sincere thanks to all the faculty members including technical staff of the Department of Environmental Science, The University of Burdwan, for their moral support. Authors also like to thank to the technical staff of University Instrumentation Centre (USIC), The University of Burdwan, for their active help with sample characterization.

GRANT SUPPORT DETAILS

The present research did not receive any financial support.

CONFLICT OF INTEREST

The authors declare that there is not any conflict of interests regarding the publication of this manuscript. In addition, the ethical issues, including plagiarism, informed consent, misconduct, data fabrication and/ or falsification, double publication and/or submission, and redundancy has been completely observed by the authors.

LIFE SCIENCE REPORTING

No life science threat was practiced in this research.

REFERENCES

Acemioglu, B. (2004). Adsorption of Congo Red from aqueous solution onto calcium-rich fyash. J. Colloid Interface Sci. 274(2), 371–379. https://doi.org/10.1016/j.jcis.2004.03.019

Aminu, I., Gumel, S.M., Ahmad, W.A., & Idris, A.A. (2020). Adsorption Isotherms and Kinetic Studies of Congo-Red Removal from Waste Water Using Activated Carbon Prepared from Jujube Seed. Am. J. Anal. Chem. 11, 47-59. https://doi.org/10.4236/ajac.2020.111004

Bannerjee, S., & Chattopadhyaya, A.C. (2017). Adsorption characteristics for the removal of a toxic dye, tartrazine from aqueous solutions by a low cost agricultural by-product. Arabian J. Chem. 10, S1629-S1638 https://doi.org/10.1016/j.arabjc.2013.06.005

Begum, H.A., & Kabir, M.H., (2013). Removal of Brilliant Red from Aqueous Solutions by Adsorption on Fish Scales. Dhaka Univ. J. Sci. 61, 7–12.

Bhaumik, R., Mondal, N.K., Das, B., Roy, P., & Pal, K.C. (2011). Predicting iron adsorption capacity and thermodynamics onto calcareous soil from aqueous solution by linear regression and neural network modeling, Universal J. Environ. Res. Technol. 1(4), 486–499

Çelekli, A., Al-Nuaimi, A.I., & Bozkurt, H. (2019). Adsorption kinetic and isotherms of Reactive 449 Red 120 on Moringa oleifera seed as an eco-friendly process. J. Mol. Struct. 1195, 168-178.

Chowdhury, S., Chakraborty, S., & Saha, P.D. (2013). Response surface optimization of a dynamic dye adsorption process: a case study of crystal violet adsorption onto NaOH-modified rice husk. Environ. Sci. Pollut. Res. 20, 1698–1705.

Chattoraj, S., Mondal, N.K., Das, B., Roy, P., & Sadhukhan, B. (2014). Biosorption of carbaryl from aqueous solution onto *Pistia stratiotes* biomass, Appl. Water Sci. 4(1), 79–88

Dada, A.O., Olalekan, A., Olatunya, A.M., & Dada, O. (2012). Langmuir, Freundlich, Temkin and Dubinin Radushkevich isotherms studies of equilibrium sorption of Zn^{2+} unto phosphoric acid modified rice husk. J. Appl. Chem. 3, 38-45.

Das, B., & Mondal, N.K. (2011). Calcareous soil as a new adsorbent to remove lead from aqueous solution: equilibrium, kinetic and thermodynamic study. Universal J. Environ. Res. Technol. 1(4), 515–530.

Das, B., Mondal, N.K., Bhaumik, R., & Roy, P. (2013). Insight into adsorption equilibrium, kinetics and thermodynamics of lead onto alluvial soil. Int. J. Environ. Sci Technol. 73, 305-310.

Debnath, P., & Mondal, N.K. (2020). Efective removal of congo red dye from aqueous solution using biosynthesized zinc oxide nanoparticles. Environ. Nanotechnol. Monit. Manag. 14,100320.

Dryaz, A.R., Shaban, M., AlMohamadi, H., Khulood, A., Abu Al-Ola, Hamd, A., Soliman, N.K., Sayed, A., & Ahmed, S.A. (2021). Design, characterization, and adsorption properties of Padina gymnospora/zeolite nanocomposite for Congo Red dye removal from wastewater. Sci Rep 11:21058. https://doi.org/10.1038/s41598-021-00025-y.

Govindaraj, P., Gnanavelraja, N., Subramanian, T., & Balji, B.G. (2018). Eco-friendly method to detoxify dyes from textile efuent using bricks kiln chamber fly ash as adsorbent. Int. J. Appl. Eng. Res. 13(14), 11693-11700.

Guo, Y., Qi, J., Yang, S., Yu, K., Wang, Z., & Xu, H. (2002). Adsorption of Cr(VI) on micro and mesoporous rice husk-based active carbon. Mater. Chem. Phys. 78(1), 132–137.

Gurav, R., Bhatia, S.K., Choi, T-R., Choi, Y-K., Kim, H.J., Song, H-S., Lee, S.M., Park, S.L., Lee, H.S., Koh, J., Jeon, J-M., Yoon, J-J., & Yang, Y-H. (2021) Application of macroalgal biomass derived biochar and bioelectrochemical system with Shewanella for the adsorptive removal and biodegradation of toxic azo dye. Chemosphere 264(2), 128539, https://doi.org/10.1016/j.chemosphere.2020.128539

Harja, M., Buema, G., & Bucur, D. (2022). Recent advances in removal of Congo Red dye by adsorption using an industrial waste. Sci. Rep. 12, 6087. https://doi.org/10.1038/s41598-022-10093-3

Harja, M.http://www.pjoes.com/Author-Van Tan-Lam/141238, Buema, G., & Bucur, D. (2022). Recent advances in removal of Congo Red dye by adsorption using an industrial waste. Sci. Report 12, 6087. https://doi.org/10.1038/s41598- 022-10093-3

Lam, V.T., Dao, To-Uyen. T., Nguyen, H-T. T., Nguyen, D.T.C., Le, H.T.N., Nguyen, H.T.T., Do, Sy T., & Loc, H.H. (2021). Process Optimization Studies of Congo Red Dye Adsorption onto Magnesium Aluminium Layered Double Hydroxide Using Response Surface Methodology. Pol. J. Environ. Stud. 30(1), 679–687. https://doi.org/10.15244/pjoes/121048

Harja, M., Lupu, N., Chiriac, H., Herea, D-D., & Buema, G. (2022). Studies on the Removal of Congo Red Dye by an Adsorbent Based on Fly-Ash@Fe_3O_4 Mixture. Magnetochem. 8, 125. https://doi.org/10.3390/ magnetochemistry8100125

Han, M., Xu, B., Zhang, M., Yao, J., Li, Q., Chen, W., & Zhou, W. (2021). Preparation of biologically reduced graphene oxide-based aerogel and its application in dye adsorption. Sci. Total Environ. 783, 147028. https://doi.org/10.1016/j.scitotenv.2021.147028

Islam, M.A., Ali, I., Karim, S.M.A., Firoz, H.M.S., Chowdhury, A-N., Morton, D.W., & Angove, M.J. (2019). Removal of dye from polluted water using novel nano manganese oxide-based materials. J. Water Process Eng. 32, 100911. https://doi.org/10.1016/j.jwpe.2019.100911.

Jaafar, A., Darchen, A., Driouich, A., Lakbaibi, Z., Boussaoud, A., Chatib, B., Laftani, Y., Makhfouk, M.El., & Hachkar, M. (2022). Fish scale of *Sardina pilchardus* as a biosorbent for the removal of Ponceau S dye from water: Experimental, designing and Monte Carlo investigations. Inorg. Chem. Commun. 137, 109196. https://doi.org/10.1016/j.inoche.2022.109196

Januário, E.F.D., Vidovix, T.B., de Camargo Lima, B.N., Paixão, R.M., da Silva, L.H.B.R., Homem, N.C., Bergamasco, R., & Vieira, A.M.S. (2021). Advanced graphene oxide-based membranes as a potential alternative for dyes removal: A review. Sci. Total Environ. 789, 147957. https://doi.org/10.1016/j.scitotenv.2021.147957.

Jabar, J.M., Odusote, Y.A., Alabi, K.A., & Ahmed, I.B. (2020). Kinetics and mechanisms of congo-red dye removal from aqueous solution using activated *Moringa oleifera* seed coat as adsorbent. Appl. Water Sci. 10, 136 (2020). https://doi.org/10.1007/s13201-020-01221-3

Jawad, A.H., & Abdulhameed, A.S. (2020). Mesoporous Iraqi red kaolin clay as an efficient adsorbent for methylene blue dye: Adsorption kinetic, isotherm and mechanism study. Surf. Interfaces 18, 100422. https://doi.org/10.1016/j.surfin.2019.100422.

Kabir, S.M.F., Cueto, R., Romeo, S.L.D.B., Kuttruff, J.T., Marx, B.D., & Negulescu, I.I. (2019). Removal of Acid Dyes from Textile Wastewaters Using Fish Scales by Absorption Process. Clean Technol. 1, 311-324. doi:10.3390/cleantechnol1010021

Khedmati, M., Khodaii, A., & Haghshenas, H.F. (2017). A study on moisture susceptibility of stone matrix warm mix asphalt. Constr Build. Mater. 144, 42–49. https://doi.org/ 10.1016/j.conbuildmat.2017.03.121.

Karimifard, S., & Moghaddam, M.R.A. (2018). Application of response surface methodology in physicochemical removal of dyes from wastewater: A critical review. Sci. Total Environ. 640-641, 772-797. https://doi.org/10.1016/j.scitotenv.2018.05.355.

Karaman, C., Karaman, O., Show, P-L., Karimi-Maleh, H., & Zare, N. (2022). Congo red dye removal from aqueous environment by cationic surfactant modified-biomass derived carbon: Equilibrium, kinetic, and thermodynamic modeling, and forecasting via artificial neural network approach. Chemosphere 290, 133346. https://doi.org/10.1016/j.chemosphere.2021.133346.

Kim, E-J., Bhatia, S.K., Song, J.H., Yoo, E., Jeon, J.H., Yoon, J-Y., Yang, Y., Gurav, R., Yang, Y-H., Kim, J.H., & Choi, Y-K. (2020). Adsorptive removal of tetracycline from 467 aqueous solution by maple leaf-derived biochar. Bioresour. Technol. 123092

Kumar, M.P.S., & Phanikumar, B.R. (2013). Response surface modelling of Cr^{6+} adsorption from aqueous solution by neem bark powder: Box–Behnken experimental approach. Environ. Sci. Pollut. Res. 20, 1327–1343.

Mall, I.D., Srivastava, V.C., Agarwal, N.K., & Mishra, I.M. (2005). Removal of Congo Red from aqueous solution by bagasse fly ash and activated carbon: Kinetic study and equilibrium isotherm analyses. Chemosphere 61(4), 492–501. https://doi.org/10.1016/j.chemo sphere.2005.03.065.

Mall, I.D., Srivastava, V.C., Agarwal, N.K., & Mishra, I.M. (2005). Removal of Congo Red from aqueous solution by bagasse fly ash and activated carbon: Kinetic study and equilibrium isotherm analyses. Chemosphere 61(4), 492–501. https://doi.org/10.1016/j.chemosphere.2005.03.065

Marrakchi, F., Ahmed, M.J., Khanday, W., Asif, M., & Hameed, B. (2017). Mesoporous carbonaceous material from fish scales as low-cost adsorbent for reactive orange 16 adsorption. J. Taiwan Inst. Chem. Eng. 71, 47–54.

Mondal, N.K., Roy, P., Sen, K., Mondal, A., & Debnath, P. (2023). Low-cost fluoride adsorbent prepared

from renewable bio-waste: Synthesis, characterization and optimization studies. Pollution https://doi.org/10.22059/POLL.2023.351595.1699
Mondal, M.K. (2010). Removal of Pb(II) from aqueous solution by adsorption using activated tea waste. Korean J. Chem. Eng. 27(1), 144–151
Neves, C., Scheufele, F., Nardino, A., Vieira, M., da Silva, M., Módenes, A., & Borba, C. (2018). Phenomenological modeling of reactive dye adsorption onto fish scales surface in the presence of electrolyte and surfactant mixtures. Environ. Technol. 39, 2467–2483.
Nguyen, T.T.T., Hoang, D.Q., Nguyen, D.T.C., & Tran, T.V. (2022). Adsorptive Optimization of Crystal Violet Dye Using Central Composite Rotatable Design and Response Surface Methodology: Statistical Analysis, Kinetic and Isotherm Studies. Arab J. Sci. Eng. 17, 1-14. https://doi.org/10.1007/s13369-022-07391-3.
Oloo, C.M., Onyari, J.M., Wanyonyi, W.C., Wabomba, J.N., & Muinde, V.M. (2020). Adsorptive removal of hazardous crystal violet dye form aqueous solution using Rhizophora mucronata stem-barks: Equilibrium and kinetics studies. Environ. Chem. Ecotoxicol. 2, 64-72. https://doi.org/10.1016/j.enceco.2020.05.001.
Ranjan, D., Talat, M., & Hasan, S.H. (2009). Rice polish, an alternative to conventional adsorbents for treating arsenic bearing water by up–flow column method. Ind. Eng. Chem. Res. 48(23), 10180–10185.
Roy, P., Mondal, N.K., Bhattacharya, S., Das, B., & Das, K. (2014). Removal of arsenic (III) and arsenic (V) on chemically modified low-cost adsorbent: batch and column operations. Appl. Water Sci. 3, 293–309.
Roy, T.K., Mondal, N.K., & Mitra, P. (2022). Efficacy of Mn-doped ZnO towards Removal of Congo Red Dye under UV Exposure: Isotherm, Kinetics, Thermodynamics and Optimization Study. Pollution 9(2), 513-530. http://doi.org/10.22059/POLL.2022.346963.1568
Sadhukhan, B., Mondal, N.K., & Chattoraj, S. (2014). Biosorptive removal of cationic dye from aqueous system, a response surface methodological approach. Clean Technol. Environ. Policy 16, 1015–1025. https://doi.org/10.1007/s10098-013-0701-8
Sadhukhan, B., Mondal, N.K., & Chattaraj, S. (2016). Optimization using central composite design (CCD) and the desirability function for sorption of methylene blue from aqueous solution onto Lemna major. Kerbala Int. J. Modern Sci. 2(3), 145-155. https//doi.org/10.1016/jkijoms.2016.03.005
Saleh, S.M., Maarof, H.I., Rahim, S.N.S.A., & Nasuha, N. (2012). Adsorption of Congo Red onto bottom ash. J. Appl. Sci. 12(11), 1181–1185. https://doi.org/10.3923/jas.2012.1181.1185.
Saqib, A.N.S., Waseem, A., Khan, A.F., Mahmood, Q., Khan, A., Habib, A., & Khan, A.R.(2013). Arsenic bioremediation by low cost materials derived from Blue Pine (*Pinus wallichiana*) and Walnut (*Juglans regia*). Ecol. Eng. 51, 88–94 https://doi.org/10.1016/j.ecoleng.2012.12.063
Samarghandi, M.R., Hadi, M., Moayedi, S., & Askari, F.B. (2009). Two parameter isotherms of methyl orange sorption by pinecone derived activated carbon. Iran J. Environ. Health Sci. Eng. 6, 285-294.
Saravanan, A., Karishma, S., Senthil Kumar, Varjani, S.P., Yaashikaa, P.R., Jeevanantham, Ramamurthy, S.R., & Reshma, B. (2021). Simultaneous removal of Cu(II) and reactive green 6 dye from wastewater using immobilized mixed fungal biomass and its recovery. Chemosphere 271, 129519. https://doi.org/10.1016/j.chemosphere.2020.129519.
Satapathy, M., Prangya, R., Dash, R., & Aditya, K. (2020). Removal of textile 545 dyes from aqueous solutions by dolochar: equilibrium, kinetic, and thermodynamic studies. J. Hazard. Toxic Radioact. Waste 24(3), 04020015. https://doi.org/10.1061/(ASCE)HZ.2153-5515.0000509
Sen, K., & Mondal, N.K. (2022). Glyphosate adsorptive behaviour using magnetic activated carbon: kinetics, isotherms, and DFT study. Biomass Conv. Bioref . https://doi.org/10.1007/s13399-021-02193-3
Sen, K., Datta, J.K., & Mondal, N.K. (2021). Box–Behnken optimization of glyphosate adsorption on to biofabricated calcium hydroxyapatite: kinetic, isotherm, thermodynamic studies. Appl. Nanosci. 11, 687–697. https://doi.org/10.1007/s13204-020-01612-7
Sonar, S.K., Niphadkar, P.S., Mayadevi, S., & Joshi, P.N. (2014). Preparation and characterization of porous fly ash/$NiFe_2O_4$ composite: Promising adsorbent for the removal of Congo Red dye from aqueous solution. Mater. Chem. Phys. 148(1-2), 371–379. https:// https://doi.org/10.1016/j.matchemphys.2014.07.057
Vyavahare, G., Jadhav, P., Jadhav, J., Patil, R., Aware, C., Patil, D., Gophane, A., Yang, Y-H., & Gurav, R. (2019). Strategies for crystal violet dye sorption on biochar derived from mango 558 leaves

and evaluation of residual dye toxicity. J. Clean Prod. 207, 296-305. https://doi.org/10.1016/j.jclepro.2018.09.193

Vijayakumar, G., Tamilarasan, R., & Dharmendirakumar, M. (2012). Adsorption, Kinetic Equilibrium and Thermodynamic studies on the removal of basic dye Rhodamine-B from aqueous solution by the use of natural adsorbent perlite. J. Mater. Environ. Sci. 3, 157-170.

Vijayaraghavan, K., Mahadevan, A., Umid, M.J., & Balasubramanian, R. (2009). Biosorption of As(V) onto the shells of the crab (*Portunus sanguinolentus*), equilibrium and kinetic studies. Ind. Eng. Chem. Res. 48(7), 3589–3594.

Wanyonyi, W.C., Onyari, J.M., & Shiundu, P.M. (2014). Adsorption of Congo Red Dye from Aqueous Solutions Using Roots of *Eichhornia crassipes*: Kinetic and Equilibrium Studies. Energy Procedia 50, 862 – 869. https://doi.org/10.1016/j.egypro.2014.06.105

Wekoye, J.N., Wanyonyi, W.C., Wangila, P.T., & Tonui, M.K. (2020). Kinetic and equilibrium studies of Congo red dye adsorption on cabbage waste powder. Environ. Chem. Ecotoxicol. 2, 24-31. https://doi.org/10.1016/j.enceco.2020.01.004.

Witek-Krowiak, A., Chojnacka, K., Podstawczyk, D., Dawiec, A., & Pokomeda, K. (2014). Application of response surface methodology and artificial neural network methods in modelling and optimization of biosorption process. Bioresour. Technol. 160, 150–160. https://doi.org/10.1016/j.biortech.2014.01.021.

Yadav, M., Thakore, S., & Jadeja, R. (2021). Removal of organic dyes using *Fucus vesiculosus* seaweed bioadsorbent an ecofriendly approach: Equilibrium, kinetics and thermodynamic studies. Environ. Chem. Ecotoxicol. 4, 67-77. https://doi.org/10.1016/j.enceco.2021.12.003.

Yang, Y., Nguyen, T.M.P., Van, H.T., Nguyen, Q.T., Nguyen, T.H., Nguyen, T.B.L., Hoang, Le, P., Thanh, D.V., Nguyen, T.V., Nguyen, V.Q., Thang, P.Q., Yılmaz, M., & Giang, Le. V. (2022). ZnO nanoparticles loaded rice husk biochar as an effective adsorbent for removing reactive red 24 from aqueous solution. Mater. Sci. Semicond. 150, 106960. https://doi.org/10.1016/j.mssp.2022.106960.

Zhu, K., Gong, X., He, D., Li, B., Ji, D., Li, P., Peng, Z., & Luo, Y. (2013). Adsorption of Ponceau 4R from aqueous solutions using alkali boiled Tilapia fish scales. RSC Adv. 3, 25221–25230.